

Optimisation of Magnetisation Transfer Ratio sequence acquisition parameters: application to the spinal cord

Marco Battiston¹, James E M Fairney^{2,3}, Marios C Yiannakas¹, Claudia A M Wheeler-Kingshott¹, and Rebecca S Samson¹

¹NMR Research Unit, Department of Neuroinflammation, Queen Square MS Centre, UCL Institute of Neurology, London, England, United Kingdom, ²Department of Medical Physics and Biomedical Engineering, UCL, London, England, United Kingdom, ³Department of Brain Repair and Rehabilitation, UCL Institute of Neurology, London, England, United Kingdom

Target audience: Scientists and clinicians interested in spinal cord Magnetisation Transfer Imaging methods.

Purpose: To optimise a Magnetisation Transfer Ratio acquisition protocol with respect to sensitivity to the bound pool fraction (BPF). **Introduction:** The spinal cord (SC) is affected in neurological disorders, with abnormalities detected both in cord white (WM) and grey matter (GM)¹. Magnetisation Transfer (MT) imaging techniques are sensitive to brain and SC pathology, and the MT ratio (MTR) has been shown to be decreased in the SC in multiple sclerosis², and spinal cord injury³. However, making quantitative measurements in the SC *in vivo* is challenging due to its small cross-sectional size and the potential for SC motion during scans. Additionally, the MTR is highly sequence-dependent, and is also influenced by effects other than MT exchange, such as T_1 relaxation. Improvements in terms of image quality and acquisition time in MT imaging of the SC have been achieved by combining off-resonance saturation, by means of a train of MT RF pulses, with an EPI-based reduced field-of-view (FOV) imaging technique, such as ZOOM-EPI⁴. We aimed to optimise the off-resonance saturation parameters in an EPI-based MT sequence to maximise the sensitivity of the MTR to the BPF, considered to be a biomarker of tissue macromolecular content and attributed to myelin in the brain and SC⁵. Numerical simulations were used to determine combinations of sequence parameters (pulse maximum amplitude B_1 , frequency offset Δ , pulse duration τ , pulse repetition time PRT, and total number of pulses N) that maximised the sensitivity of the MTR to changes in the BPF, whilst simultaneously minimising MTR sensitivity to T_1 relaxation (a competing effect). An optimal and a non-optimal protocol suggested from the results of the simulations were compared in terms of MTR contrast both in Bovine Serum Albumin (BSA) phantoms and *in vivo* SC data. **Methods:** *Simulations:* Simulated MTR values were generated using the two-pool Minimal Approximation MT (MAMT) model⁶ to effectively take into account the shape and timing of the off-resonance RF pulse train. Different model configurations were created by varying BPF and free pool longitudinal relaxation rate (R_1^f) over a range of 10 linearly spaced physiologically plausible values (BPF from 0.07 to 0.19, R_1^f from 0.85s⁻¹ to 1.7s⁻¹), with other parameters fixed ($R_1^b=1\text{ s}^{-1}$, $T_2^b=50\text{ ms}$, $T_2^a=12\mu\text{s}$, $R=20\text{s}^{-1}$)⁷. For each configuration, the MTR value was simulated over all possible combinations of sequence parameters, allowed to vary as follows: B_1 from 1.5 μT to 11 μT (20 points), Δ from 1kHz to 15kHz (20 points), τ from 5ms to 30ms (15 points), PRT from 30ms to 100ms (15 points), and N = [10, 15, 20, 30, 50, 150]. The Sinc-Gaussian MT pulse shape was reproduced for the purpose of the simulations. MTR sensitivity to BPF ($\partial\text{MTR}/\partial\text{BPF}$) and R_1^f ($\partial\text{MTR}/\partial R_1^f$) was approximated by calculating the rate of change in the MTR with respect to the change in tissue parameter values, e.g. $\Delta\text{MTR}/\Delta\text{BPF}$, $\Delta\text{MTR}/\Delta R_1^f$, and averaging over all the steps in BPF and R_1^f vectors. Optimal and non-optimal MT saturation schemes were selected for comparison (taking into consideration the clinical feasibility of incorporating acquisition parameters). *Phantoms and healthy volunteer experiment:* All scanning was performed using a 3T Philips Achieva MRI system (Philips Healthcare, Best, The Netherlands) with a 32-channel head coil. An optimal and a non-optimal sequence were compared in 2 45ml BSA phantoms of concentration 20% and 25%, to mimic two tissue types with differing BPF values. A multi slice MTR sequence with single-shot EPI readout was used (6 slices, FOV=72x48mm², voxel size=1x1x5mm³, TE=30ms, NSA=4). The same protocols were tested in a healthy subject, using a single-shot ZOOM-EPI readout (6 axial slices, FOV=50x36mm² centered at C2 and covering the C1-C2 levels of the cervical cord, inner-volume thickness=39mm, TE=25ms, voxel size=0.6x0.6x5mm³, SENSE factor=1.5 in the A/P direction, halfscan factor=0.612, NSA=8). The protocols were compared in terms of MTR contrast-to-noise ratio (CNR) between different tissue types (i.e. different BSA concentration, or manually drawn whole cord WM and GM regions-of-interest). **Results:** *Simulations:* Using a saturating RF pulse train long enough to drive the system into a steady state, $\partial\text{MTR}/\partial\text{BPF}$ and $\partial\text{MTR}/\partial R_1^f$ assume analogue trends over the whole space of variability of sequence parameters. If the system is not in the steady state, $\partial\text{MTR}/\partial\text{BPF}$ can be increased and $\partial\text{MTR}/\partial R_1^f$ jointly decreased by reducing the PRT. A compromise with regards to SNR in the resulting MTR maps is observed with increasing τ . This behaviour is enhanced when N is progressively reduced (figure 1). The optimal and non-optimal protocol acquisition details chosen from simulations are reported in table 1. Non-optimal parameters were chosen to resemble those typically used in an MTR protocol, and to match the SNR in the resulting MTR maps according to simulations. *Phantoms experiment:* Example MTR maps in the BSA phantoms for the non-optimal and optimal sequence are shown in figure 2. MTR contrast between different BSA concentration phantoms is enhanced using the optimal sequence (global CNR=4.74) compared with the non-optimal (global CNR=1.42). *In vivo experiment:* Figure 3 shows SC MT_{off}, MT_{on} and MTR maps in the central slice for the non-optimal and optimal sequence. The MTR map obtained from the optimal protocol appears less noisy and, quantitatively, MTR contrast between WM and GM is increased (CNR=0.87 vs CNR=1.35). **Discussion:** We have demonstrated that the competing effects of MT and T_1 relaxation in the MTR can be disentangled when off-resonance saturation pulses are optimised. Interestingly and counter-intuitively, shorter pulse trains are a better option to achieve this. We have proposed an optimisation of the MTR using an EPI-based sequence that provides improved sensitivity to the BPF. As no cost function is minimised, the sequence proposed has been improperly defined as optimal, and other combinations of sequence parameters can provide similarly improved sensitivity, as suggested by simulations (figure 1). Optimisation of sequence parameters to maximise WM/GM MTR contrast has previously been proposed⁸. However, in this work no approximations of the two-pool model equations have been made and all sequence parameters are taken into account in the analysis. Moreover, we showed that the enhanced WM/GM contrast in MTR map can be achieved as a consequence of the improved MTR sensitivity to BPF changes. This optimisation of the EPI-based MTR sequence is of particular interest for SC applications where the ZOOM-EPI sequence can be beneficial to reduce acquisition time. **Conclusion:** MT sequence parameters can be optimised to improve the sensitivity of MTR maps to BPF while reducing the confounding effect of T_1 relaxation.

non-optimal	optimal
B_1 [μT]	6.55
Δ [kHz]	1.33
τ [ms]	13.9
PRT [ms]	80
N	48
TR [ms]	8800
$B_{1\text{rms}}$ [μT]	1.32
	5.86
	2.711
	30
	30
	15
	1.02

Table 1: non optimal and optimal parameters from simulations.

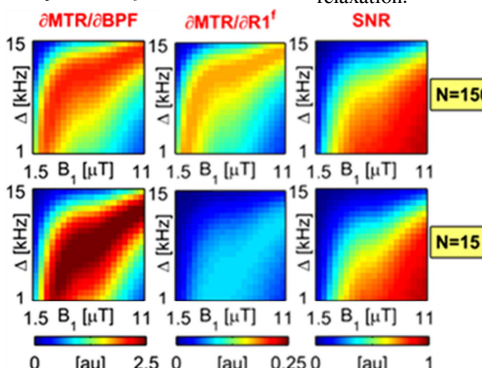


Figure 1: Simulated MTR sensitivity to BPF and R_1^f maps, and SNR map as function of B_1 and Δ , for $\tau=30\text{ms}$, PRT=30ms and N=150 to allow the steady state (top) or N=15 (bottom).

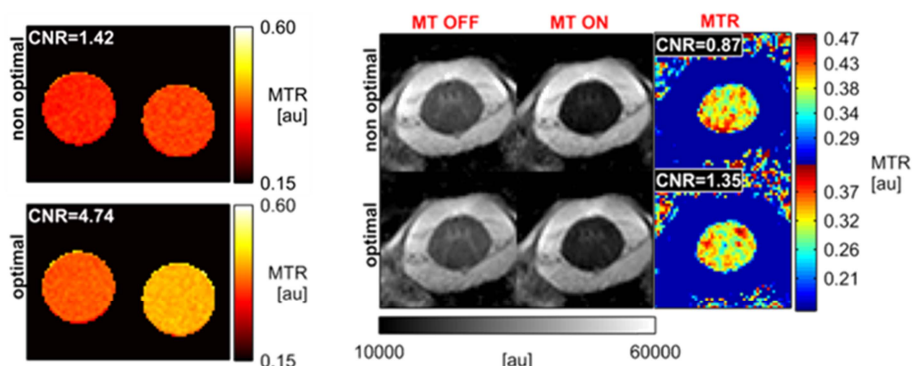


Figure 2: Example of non optimal (top) and optimal (bottom) MTR maps for phantoms experiment.

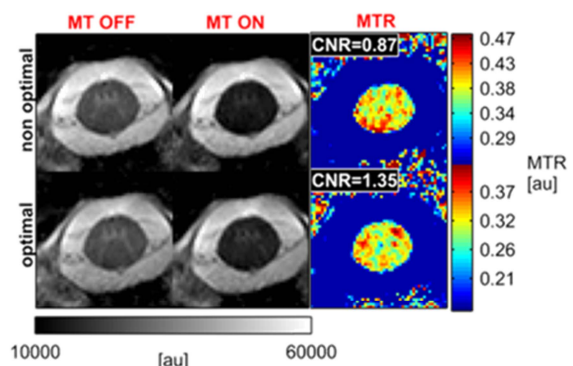


Figure 3: Example of *in vivo* SC MT_{off}, MT_{on}, and MTR images for non optimal (top) and optimal (bottom) protocol. Scales in MTR maps span the same percentiles in the intensity histograms.

References: [1] Gilmore CP *et al* Mult Scler (2009);15:180-8. [2] Filippi M *et al* Neurology (2000);54:207-13. [3] Cohen-Adad J *et al* NeuroImage (2011);55:1024-33. [4] Samson RS *et al* Proc ISMRM 2012. [5] Schmierer K *et al* JMRI (2007);26:41-51. [6] Portnoy S *et al* MRM (2007);58:144-55. [7] Sled JG *et al* MRM (2001);46:923-31. [8] Cercignani M *et al* NeuroImage (2006);31:181-6. **Acknowledgements:** We thank the MS Society of the UK for funding. This work was undertaken at UCLH/UCL who received a proportion of funding from the Department of Health's NIHR Biomedical Research Centres funding scheme. JF is funded by the MRC Training grant reference: MR/J500422/1.